Polar KTaO$_3$ surface reconstruction mediated by cation exchange unravelled by global optimisation

Daniel E. E. Deacon-Smith*, David O. Scanlon, C. Richard
A. Catlow, Alexey A. Sokol, and Scott M. Woodley*

University College London, Kathleen Lonsdale Materials Chemistry,

20 Gordon Street, London WC1H 0AJ, United Kingdom

(Dated: August 16, 2013)

KTaO$_3$, a I-V ABO$_3$ perovskite, is attracting substantial interest following the discovery of a two-dimensional electron gas (2DEG) on its (001) surface [1, 2]. Little is, however, known of its surface structure unlike the widely studied II-IV, SrTiO$_3$ counterpart [3, 4]. The polar (001) KTaO$_3$ surface, with alternating $+1$ and -1 charged terminating planes *must* undergo a reconstruction to become stable. Here, we reveal a new stabilisation mechanism which involves K enrichment of the surface in agreement with experiment [5–7]. Reconstructions of the TaO$_2$ terminated surface with inter-planar cation exchange result in stable configurations, in which highly charged Ta is fully co-ordinated and only K is exposed on the surface. A global optimisation yields a number of low-energy minimum (2 x 2) reconstructions mediated by this mechanism. We propose that this mechanism is general to polar I-V perovskite surfaces and that it will give rise to novel surface electronic properties.

Perovskite oxides attract widespread and growing interest owing to the unique electronic properties they exhibit in heterostructure interfaces and thin films, such as giant magneto resistance, high temperature superconductivity, multiferroicity, transparency, and large temperature dependent dielectric constants [8–13]. These properties give the materials great potential in the emerging field of oxide electronics, allowing creation of tuneable dielectric capacitors and nano-sized transistors [14, 15]. With the recent discovery of 2DEGs on the cleaved (001) surfaces of KTaO$_3$ and SrTiO$_3$, perovskite surfaces are now the focus of much increased attention [1, 2, 16, 17].

KTaO$_3$ is a cubic perovskite at all temperatures, consisting of TaO$_6$ corner sharing octahedra, with K occupying the large 12-fold coordinate sites [18]. The formal charges for K, Ta, and O are $+1$, $+5$, and -2 respectively, and thus along the (001) direction there are alternating charged planes of KO $^{-1}$ and TaO$_2$ $^{+1}$ (Fig. 1), leading to a stoichiometric slab possessing a "Tasker type 3" polar surface, which is unstable, and must undergo reconstruction [19].

At present, however, the precise experimental structure of (001) KTaO$_3$ surface is still uncertain. Helium atom scattering experiments have revealed that initially after cleaving, metastable surfaces appear, eventually decaying to a (1x1) surface, probably due to the formation of vacancies [6, 7]. Secondary ion mass spectrometry has shown that in the near surface region, KO is dominant at the surface, while TaO$_2$ is more abundant in the deeper sub-layers. Migration of K ions towards the surface, and Ta ions towards the bulk, are

2

the suggested mechanisms leading to this surface stoichiometry. Density functional theory (DFT) calculations reported a KO terminated (2x1) terraced surface to be the most stable for stoichiometric KTaO$_3$ [20]. For such a complex system, however, it is essential to explore systematically a full range of structural possibilities to establish a robust and reliable model.

Here we report a new surface stabilisation mechanism, supported by a range of reconstructions of the 2x2 stoichiometric KTaO$_3$ (001) surface, which are more stable than any previously predicted. Our approach consists of using the combination of atomistic level simulations using interatomic potentials, with the lowest energy configurations being refined by DFT. By performing a global structure optimisation of the KTaO$_3$ surface, we show that a reconstruction of the TaO$_2$ terminated surface, results in a set of surfaces that are more stable than any reconstructions of the KO terminated surface, including those discussed previously [20]. For both terminations the topmost surface layer however, consists of KO units, consistent with experimental reports. To be consistent with the TaO$_2$ termination, K ions migrate upwards from the sub-surface into the surface layer, while TaO units descend from the surface into the sub-surface layer. The mechanism is driven by the migration of the highly charged Ta cation from the surface to the bulk where it gains a higher co-ordination. This mechanism is, we suggest, general in surface reconstructions, leading to the most stable surface reconstructions of materials that possess cations whose charges differ greatly [21].

For atomistic simulations, we employ specifically designed interatomic potentials (IP) with parameters fitted using the General Utility Lattice Program (GULP) [22] (see Supplementary Information). The IPs allowed us to screen the vast number of possible surface arrangements created by our in-house global optimisation code, the Knowledge Led Master Controller (KLMC), and identify the stable configurations (see Supplementary Information).

The global optimisation revealed that the most stable structures of the TaO$_2$ terminated surface, have lower surface energies than those of the KO termination (Fig. 2). The energetically most favourable reconstructions of the half TaO$_2$ surface involved a rearrangement of both the upper and lower surface layer. In the support layer, every other chain of K ions is replaced by a TaO chain, so the 2x2 KO bulk plane is transformed into alternating 2x1 strips of bulk-like KO and TaO$_2$ (Fig 3). The remaining O ions cap the underlying Ta, so forming chains in the upper surface layer, whereas the K ions occupy sites at a maximum distance from cations in the sub-layer and with a maximum number of nearest neighbour O ions. The KO slab reconstructions resulted in rearrangements of only the surface layer, the
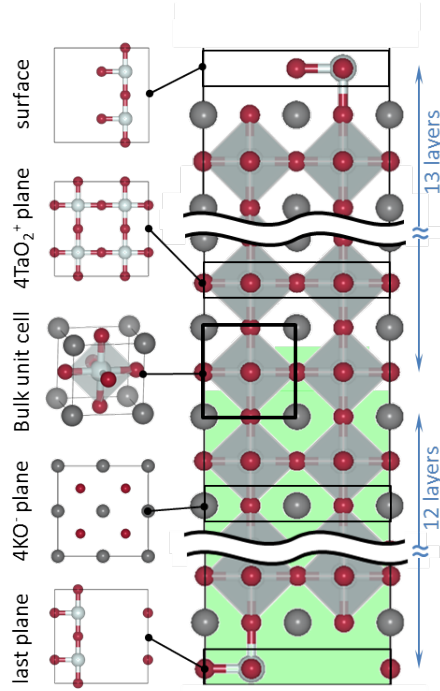
FIG. 1: **Slab Model**. An example model of a (001) KTaO$_3$ surface using a slab in which the dipole has been removed. Also highlighted are the alternating charged layers and the structure of the bulk unit cell.

initial sub-surface layer proving the most stable.

Our IP search produced two stable arrangements of the surface atoms for the TaO$_2$-terminated surface reconstruction, the K cornered and island surface arrangements (Fig. 2(c and e)). For the KO-terminated surface there are four stable arrangements: the K-cornered chain, the island, the O-cornered chain, and the diagonal surface arrangements (Fig. 2(f,g,h,j)).

The KO bulk-like, terraced surface layer (Fig. 2(e and i)), was found to be unstable with the interatomic potentials, and when relaxed adopted the K-cornered chain arrangement [20]. We note that when analysing a 2x1 surface, the KO bulk-like surface may appear as stable, as the symmetry breaking of the K cornered surface cannot take place on a 2x1 surface, which is indeed applicable to all of our non-bulk-like surfaces. Phonon calculations on the K cornered surface show a low frequency surface mode, with surface K ions vibrating in the direction that would lead to a phase transition between our ground state and the KO bulk-like surface.
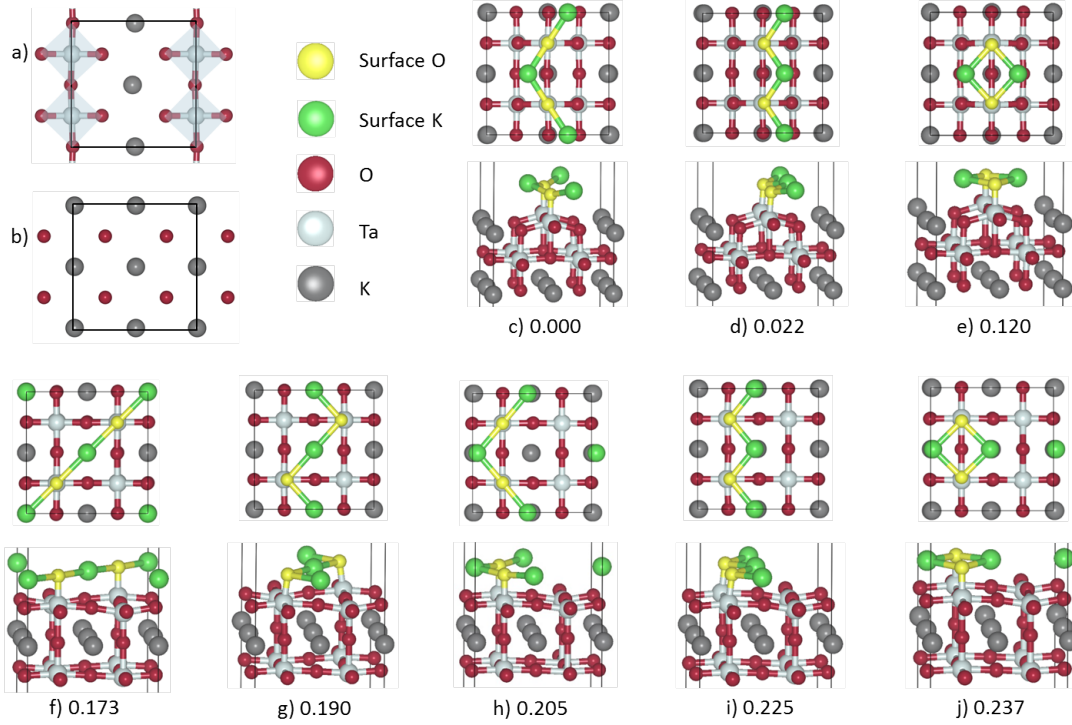
FIG. 2: **KTaO$_3$ surface structures**. (a) The mixed sub surface layer obtained by the reconstruction of the TaO2 terminated surface; (b) pure sub surface layer of the ideal TaO$_2$ termination; (c-j) eight candidate surface models after DFT relaxation (the top and side views). TaO2 terminated surfaces shown in (c-e) where the top most surface layer (TaO$_2$) has mixed with the sub layer (KO), resulting in a new external layer of KO, and a mixed sub layer highlighted in (a), consisting of rows of both TaO$_2$ and KO. The atomic arrangement of the sub layer is consistent for all three surfaces. In the external layer the position of the O does not differ, always directly above the Ta in the layer below. These surface models differ only in the arrangement of the K around the O. (f-j) are reconstructions of the KO terminated surface. In these models the sub layer is an unchanged bulk TaO$_2$ layer. The O ions in the external layer are again positioned directly above the Ta, however, there are now four possible sites, allowing a more diverse range of surface structures. The K ions are positioned around the O. In total there, are five unique external layers labelled: (c,h) K-cornered chains, (d,i) bulk terraced, (e,j) island, (g) O-cornered chains, (f) diagonal. Surface energies are relative to the groundstate. The ground state energy was found to be 0.871 Jm^{-2}.
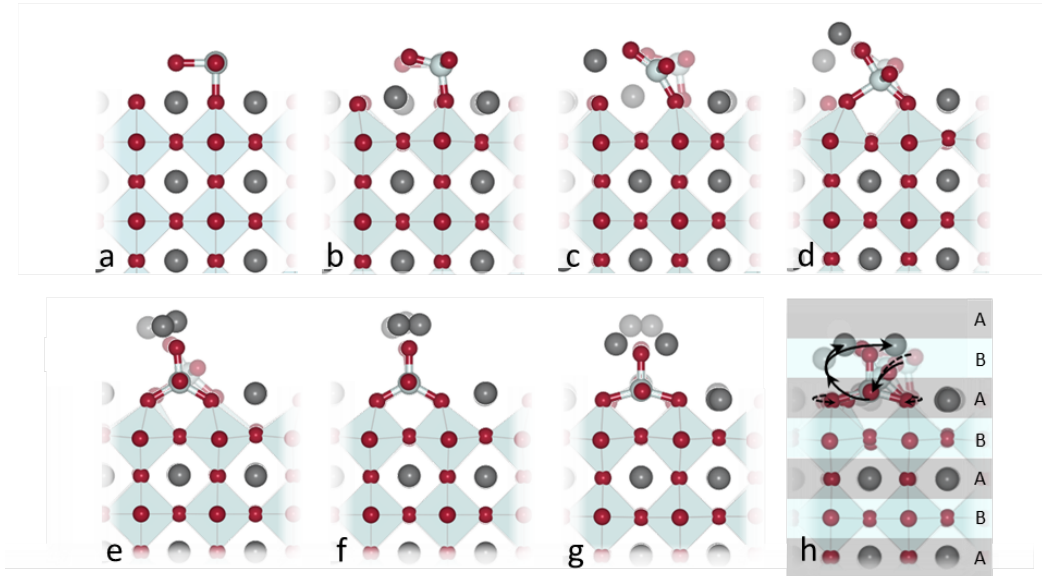
FIG. 3: **Reconstruction mechanism**. Proposed mechanism for the reconstruction of the Ta terminated (001) surface, with K migrating towards the surface, and Ta falling into the sub layer. (a) starting bulk terminated configuration. (b-g) snap shots with a shadow of the previous frame, with (g) the final DFT relaxed structure. (h) the overall DFT transition, where A and B cation layers are shaded differently.

In our DFT calculations the eight surface structures - six of which were found by our IP calculations - shown in Fig. 2 have been relaxed using DFT, in the Vienna Ab initio Simulation Package (VASP) [23, 24], details can be seen in the Supplementary Information. The DFT calculations support the results of our interatomic potential calculations, in that the surfaces with the mixed sub-layer - initially TaO_2 terminated - are lower in energy than surfaces with the TaO_2 sub-layer. While the bulk-like KO terrace surface is stable, and sits in a potential energy well, the K cornered surface structure to which they relax when using the IP methods is shown to be energetically more favourable.

A feature present in all of these surfaces is that the surface oxygen ions always sit on top of the tantalum in the sub layer. Previous work on the structure prediction of clusters [25] has shown that given the opportunity, higher charged cations maximise their coordination before the lower charged cations. This leads to the higher charged cations located nearer the centre of clusters, where as the lower charge cations are forced to take up positions close to

6

the surface. Applying this rationale, it is then unsurprising that the TaO_2-bulk terminated surface, reconstructed in a way such that the tantalum descends into the bulk to become fully coordinated, and that the stable surface arrangements all have oxygen above tantalum instead of potassium. Moreover, the diagonal and O-cornered chain surfaces are not stable on the mixed sub-layer, as these surfaces would be terminated by under-coordinated Ta ions, despite there being enough surface O ions to give a full Ta co-ordination. For the KO bulk terminated surface we have found five stable surfaces (Fig. 2(f-j)). The diagonal and O-cornered chain structures are possible on this surface due to there now being four Ta ions in the layer below, and thus the O^{2-} are no longer confined to sit on the same row. The difference in stability of these five surfaces can be attributed to the distances and shielding between the like ions, with the O ions distance being slightly more significant due to its higher charge. However, the effect of filling the Ta co-ordination dwarfs that of the topmost surface layer arrangement, as all of the mixed sub layer surface reconstructions are lower in energy. Thus we suggest that the driving mechanism for stabilisation of the surface, is the maximising of the Ta co-ordination due to the large charge disparity between Ta and K.

Turning our attention to the more general area of (I-V) perovskites we highlight a number of experimental reports where (001) or (110) surfaces have been found rich in group 1 elements ([26, 27]). Although the generic behaviour of smaller and higher charged cations to move into the bulk, away from the surface, and their drive for an increase in co-ordination are well established [21, 28], the realisation of their potential for cation exchange with more labile species - such as light alkali ions - in the sub-surface regions is identified here as the primary mechanism in the stabilisation of these materials.

To facilitate future experimental analysis, we have produced simulated Scanning Tunnelling Microscopy images (Fig. 4) of three surfaces, the ground state and the KO bulk-like surface arrangements on both of our stable sub layers. There are presently no high resolution experimental STM results of the $KTaO_3$ (001). The STM images are plotted as the charge density of the electronic states close to the Fermi level, which are probed in experiment. The images highlight the difficulty in trying to distinguish between the two KO bulk-like terminated surfaces (Fig. 4(b,c)) by STM alone despite the differing sub layers, but highlight the difference in the charge distribution between our ground state (Fig. 4(a)) and the other surface arrangements.

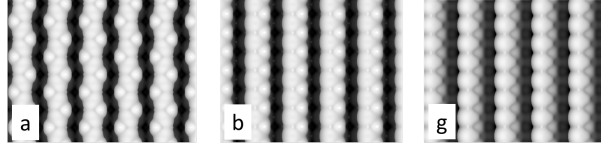Tracking the variation in the electronic band structure projected on the layers, from

FIG. 4: **STM images**. Simulated STM images of surfaces (a,b,g) in Fig. 2. The brightness indicates the distance from the tip. The images were created by looking at constant charge density levels close to the top of the valence band [29].

bulk to the surface, we observe a pronounced upwards band bending of the conduction band (see Supplementary Information), which by itself could only lead to hole accumulation at the surface rather than electrons. However, considering the valence band behaviour we observe a peculiar destabilization of oxygen localized states in the mixed sublayer of our lowest energy reconstructed surface models. This unusual feature would result in a stabilization of oxygen vacancies in the sublayer, thus generating an essential electron reservoir [30], observed as a 2DEG in $KTaO_3$, which is currently under investigation.

In conclusion, using global optimisation techniques, we have uncovered a range of surface arrangements for the stoichiometric (001) $KTaO_3$ surface lower in energy than those previously modelled. This includes a new ground state with a surface energy of 0.871 Jm^{-2}, which is 0.225 Jm^{-2} lower in energy than the currently assumed ground state. We propose that the mechanism for the stabilisation of $KTaO_3$ is driven by the maximising of the Ta co-ordination, due to the large charge disparity between Ta and K. This factor causes the Ta to descend into the bulk for TaO_2 terminated surfaces, while K migrates to the surface. We suggest this to be a general result, applicable to all (I-V) perovskites, and possibly other layered materials possessing cations of greatly differing charges.

––––––––––

[1] King, P. D. C. *et al.* Subband structure of a two-dimensional electron gas formed at the polar surface of the strong spin-orbit perovskite $KTaO_3$. *Physical review letters* **108** (2012).

[2] Santander-Syro, A. F. *et al.* Orbital symmetry reconstruction and strong mass renormalization in the two-dimensional electron gas at the surface of $KTaO_3$. *Physical Review B* **86**, 121107 (2012).

[3] Enterkin, J. A. *et al.* A homologous series of structures on the surface of $SrTiO_3(110)$. *Nature*

Materials **9**, 245–248 (2010).

[4] Zhu, G.-z., Radtke, G. & Botton, G. A. Bonding and structure of a reconstructed (001) surface of SrTiO$_3$ from TEM. *Nature* **490**, 384–387 (2012).

[5] Szot, K. *et al.* Chemical inhomogeneity in the near-surface region of KTaO$_3$ evolving at elevated temperatures. *Journal of Physics: Condensed Matter* **12**, 4687–4697 (2000).

[6] Li, J. A. *et al.* Observation of a metastable periodic structure for the (001) surface of KTaO$_3$ after cleaving in situ. *Physical Review Letters* **86**, 4867–4870 (2001).

[7] Li, J. A. *et al.* Surface structure and dynamics of KTaO$_3$(001). *Physical Review B* **68**, 045402 (2003).

[8] Müller, K. A. & Burkard, H. SrTiO$_3$: an intrinsic quantum paraelectric below 4 K. *Physical Review B* **19**, 3593–3602 (1979).

[9] Sirenko, A. A. *et al.* Soft-mode hardening in SrTiO$_3$ thin films. *Nature* **404**, 373–376 (2000).

[10] Maignan, A., Simon, C., Caignaert, V. & Raveau, B. Giant magnetoresistance ratios superior to 1011 in manganese perovskites. *Solid State Communications* **96**, 623–625 (1995).

[11] Wu, M. K. *et al.* Superconductivity at 93 k in a new mixed-phase y-ba-cu-o compound system at ambient pressure. *Physical Review Letters* **58**, 908–910 (1987).

[12] Dong, S. & Liu, J.-M. Recent progress of multiferroic perovskite manganites. *arXiv:1204.0577* (2012). Modern Physics Letters B 26, 1230004 (2012).

[13] Scanlon, D. O. Defect engineering of BaSnO$_3$ for high-performance transparent conducting oxide applications. *Physical Review B* **87**, 161201 (2013).

[14] Mannhart, J. & Schlom, D. G. Oxide Interfaces—An opportunity for electronics. *Science* **327**, 1607–1611 (2010).

[15] Ramirez, A. P. Oxide electronics emerge. *Science* **315**, 1377–1378 (2007).

[16] Santander-Syro, A. F. *et al.* Two-dimensional electron gas with universal subbands at the surface of SrTiO$_3$. *Nature* **469**, 189–193 (2011).

[17] Meevasana, W. *et al.* Creation and control of a two-dimensional electron liquid at the bare SrTiO$_3$ surface. *Nature Materials* **10**, 114–118 (2011).

[18] Zhang, L., Zhong, W. L., Wang, Y. G. & Wang, C. L. On the possible curie temperature and ferroelectricity for SrTiO$_3$ and KTaO$_3$. *physica status solidi (a)* **168**, 325–329 (1998).

[19] Tasker, P. Stability of ionic-crystal surfaces. *Journal of Physics C-Solid State Physics* **12**, 4977–4984 (1979).

[20] Fritsch, J. & Schroder, U. Reconstruction of the (001) surface of potassium tantalate. *Physica Status Solidi B-Basic Research* **215**, 827–831 (1999).

[21] Wolf, D. Reconstruction of NaCl surfaces from a dipolar solution to the madelung problem. *Physical Review Letters* **68**, 3315–3318 (1992).

[22] Gale, J. D. GULP: a computer program for the symmetry-adapted simulation of solids. *Journal of the Chemical Society-Faraday Transactions* **93**, 629–637 (1997).

[23] Kresse, G. & Furthmüller, J. Efficiency of ab-initio total energy calculations for metals and semiconductors using a plane-wave basis set. *Computational Materials Science* **6**, 15–50 (1996).

[24] Kresse, G. & Furthmüller, J. Efficient iterative schemes for ab initio total-energy calculations using a plane-wave basis set. *Physical Review B* **54**, 11169–11186 (1996).

[25] Woodley, S. M. Structure prediction of ternary oxide sub-nanoparticles. *Materials & Manufacturing Processes* **24**, 255–264 (2009).

[26] Szot, K. *et al.* Nature of the surface layer in ABO_3-type perovskites at elevated temperatures. *Applied Physics A* **62**, 335–343 (1996).

[27] Molak, A., Pawełczyk, M., Kubacki, J. & Szot, K. Nano-scale chemical and structural segregation induced in surface layer of $NaNbO_3$ crystals with thermal treatment at oxidising conditions studied by XPS, AFM, XRD, and electric properties tests. *Phase Transitions* **82**, 662–682 (2009).

[28] Davies, M. J., Parker, S. C. & Watson, G. W. Atomistic simulation of the surface structure of spinel. *Journal of Materials Chemistry* **4**, 813–816 (1994).

[29] Vanpoucke, D. E. P. & Brocks, G. Formation of Pt-induced Ge atomic nanowires on Pt/Ge(001): a density functional theory study. *Physical Review B* **77**, 241308 (2008).

[30] Harashima, S. *et al.* Coexistence of two-dimensional and three-dimensional Shubnikov–de Haas oscillations in Ar^+-irradiated $KTaO_3$. *Physical Review B* **88**, 085102 (2013).